Exploiting Deep Eutectic Solvents and Ionic Liquids for the Valorization of Chestnut Shell Waste

Elena Husanu,[||] Angelica Mero,[||] Jose Gonzalez Rivera, Andrea Mezzetta, Julian Cabrera Ruiz, Felicia D'Andrea, Christian Silvio Pomelli, and Lorenzo Guazzelli*

ACCESS | Metrics & More | Article Recommendations | Supporting Information

ABSTRACT: The full utilization of agricultural waste and its recycle into a new chain of value are of primary importance for the development of a sustainable and profitable agricultural industry. Chestnut shell waste (CSW) is an interesting case of study, whose valorization has been though partially investigated to date. This work aims at exploring the complete utilization of CSW, in terms of obtaining both value-added compounds and enriched cellulose and lignin fractions. The results were obtained via the unreported combined use of two classes of nonconventional organic solvents, namely natural deep eutectic solvents and bio-based ionic liquids (bio-ILs). At first, combinations of choline chloride (ChCl)-based DESs with an acid, a polyol, or a sugar as hydrogen bond donors were employed for the extraction of polyphenols from the CSW. The best performing system was found to be ChCl:oxalic acid dihydrate (ChCl:Oax2H$_2$O). The extraction efficiencies of the DESs tested correlate well with the measured Kamlet−Taft α parameters. After polyphenol removal, the residual solid material was treated with a bio-IL [cholinium glycinate (ChGly)] for further separation of lignin and cellulose. The products obtained by the fractionation process were characterized by Fourier transform infrared spectroscopy and thermogravimetric analysis, which confirmed the separation of the residue into a lignin-rich material and a cellulose-rich material. The results obtained were further corroborated by a three parallel reaction model combined with the distributed activation energy model, which allowed for predicting the composition of the pristine CSW and of the ChCl:Oax2H$_2$O-treated CSW as well as the two fractions obtained after ChGly treatment. The recyclability of the best performing DES and the recovery of the bio-IL have also been proven, which make the whole process viable and amenable for large-scale applications.

KEYWORDS: chestnut shell waste, circular bioeconomy, natural deep eutectic solvents, bio-based ionic liquids
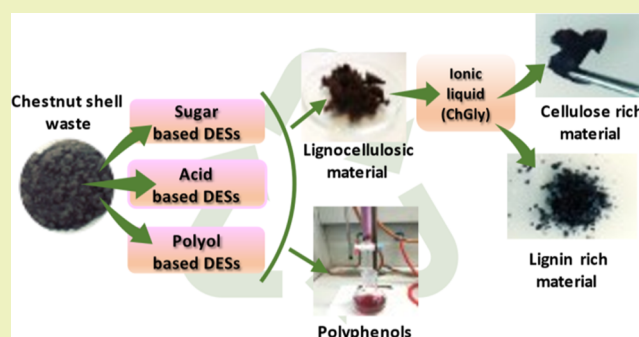
INTRODUCTION

In the food industry, residues are often solid organic matter that is typically used for composting, for animal feeding, or discarded as waste. Untoward disposal of untreated food waste, usually in open areas, can result in environmental issues.[1] In the last few years, both industry and academia have focused their attention on the extraction of high value-added compounds from food waste, which can be treasured by other industries thus creating a circular bioeconomy.[2]

Chestnut shells represent an attractive food waste that is generated in the southern part of Europe. Italy is one of the major producers of marron glacé and chestnut flour for gluten-free diets together with Portugal, Spain, and France. This industry generates several tons per year of processing wastes. Chestnut shell waste (CSW), which represents 10% of the total chestnut mass, can be regarded as a renewable raw material for the further production of new chemical entities. Indeed, several studies reported that chestnut shells as well as chestnut leaves and bur contain high levels of polyphenolic metabolites, including simple phenolic acids, flavonoids, and more complex tannins[3−5] (Figure S1, see Supporting Information). These metabolites can be used in different fields, such as wool and cotton fabrics,[6] in leather tanning, as wood adhesives,[3] and in food and cosmetic preservation as well as in the pharmaceutical industry.[7]

In addition, the CSW contains other valuable components such as cellulose, hemicellulose (Figure S2, see Supporting Information), and lignin (Figure S3, see Supporting Information), well known for their potential as precursors of platform chemicals and new biocompatible materials.[8,9] One of the main issues in the lignocellulosic-biomass waste exploitation is the removal of lignin from the matrix. Therefore,
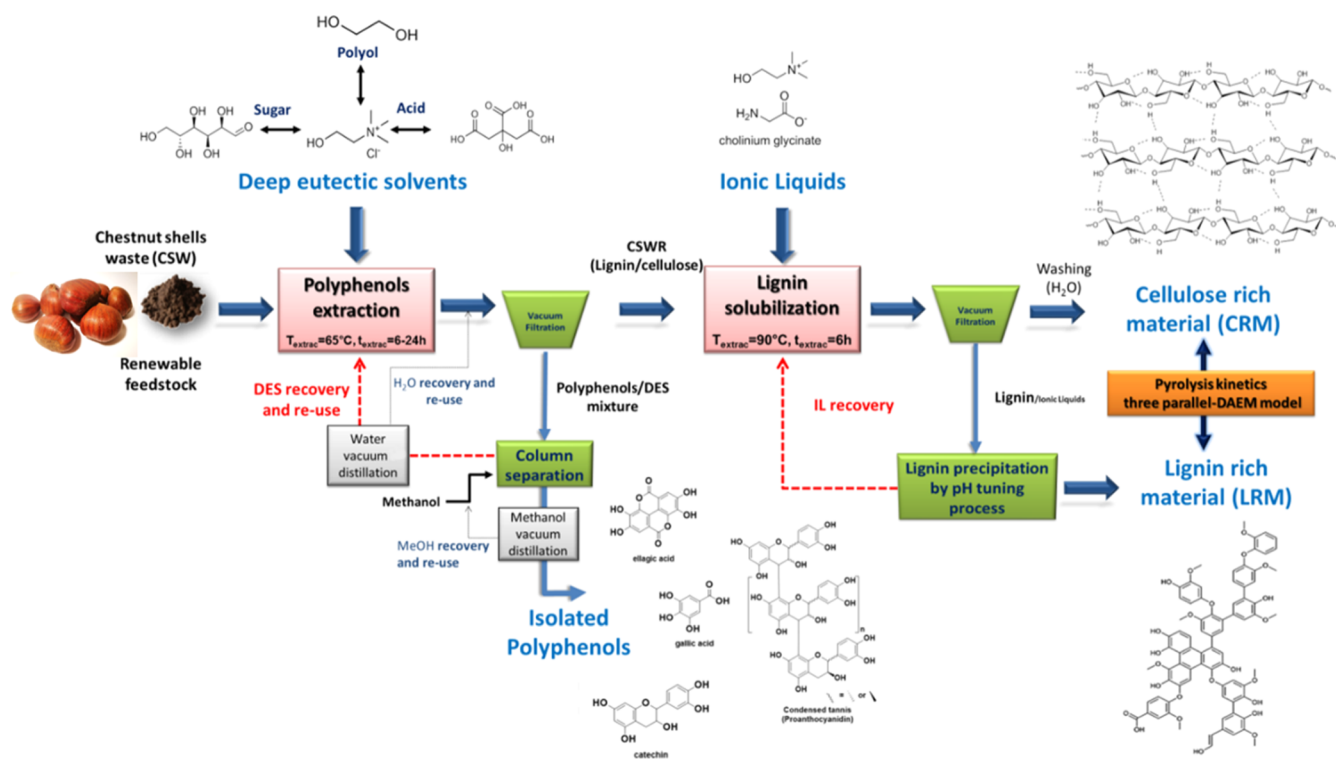
Figure 1. Scheme of the valorization of CSW.

it is crucial to develop efficient processes able to fractionate the biomass into their main components.[10]
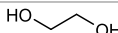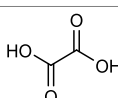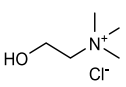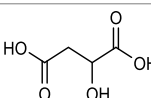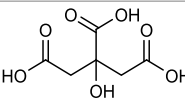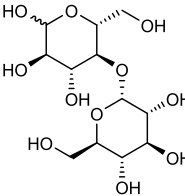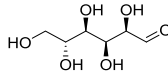
Usually, large amounts of conventional organic solvents are used for the recovery of bioactive compounds from food waste, and methanol, ethanol, ethyl acetate, and acetone have been screened in previous studies on CSW.[11] In view of developing more sustainable processes, novel and alternative solvents, endowed with environmentally friendlier profiles, are constantly sought. It is not a surprise that, for these purposes, deep eutectic solvents (DESs) have gained enormous attention in the field of extraction. Several components have been used in recent years to prepare DESs, although mixtures formed by an amine quaternary salt as a hydrogen bond acceptor (HBA) and a hydrogen bond donor (HBD) still represent one of the most common choices. To be defined as a DES, the two components must generate an eutectic mixture characterized by an eutectic point temperature lower than that of the ideal liquid mixture. Notably, such components, which can be liquids and/or solids, are mixed at a specific albeit not fixed mole ratio.[12−16] The concept of natural deep eutectic solvents (NADES) appeared in the literature for the first time in 2011. DESs having as components primary metabolites such as amino acids, organic acids, sugars, or choline derivatives belong to this class.[12,15] The recovery of bioactive compounds from different waste substrates employing DESs has been reported by several research groups.[17−21] Therefore, DESs seem to represent a step forward toward sustainable extraction processes although the full scope needs to be defined.

Another attractive class of green media is that of ionic liquids (ILs), which are organic salts with a melting point below 100 °C.[22−24] Because of their tunable, unique physiochemical properties, and solvation power, ILs have been extensively investigated as a green, and in most cases sole, class of solvent for the dissolution and fractionation of recalcitrant lignocellulosic materials. Since the initial report

from the Rogers' group,[25] several articles described the dissolution of cellulose and the treatment of biomass with various imidazolium-based ILs.[26,27] However, these ILs suffer from environmental toxicity issues.[28] As a way to overcome this limitation, a new generation of ILs obtained from natural and renewable feedstock emerged recently. These materials, called bio-based ILs (bio-ILs), were reported to be effective for the treatment of biomasses.[29−31] Indeed, readily biodegradable cholinium (Ch)—amino acid ILs[32] were successfully employed in the field of biomass treatment thanks to their low toxicity and most of all to their ability to selectively solubilize lignin from lignocellulosic materials.[33,34]

In the present study, we aimed at exploiting the resources of the CSW obtained from "Ortofrutticola Del Mugello s.r.l.", an Italian company that processes 10,000 tons/year of chestnut thus producing 700 tons/year of waste. This task was carried out via a novel two-step approach involving both types of green solvents discussed above (NADESs and bio-ILs), whose efficiency has not yet been tested on this biomass. In our intention, the combined use of these nonconventional and environmentally safer solvents would allow for the full valorization of the CSW, in contrast to most works on biomass waste valorization, which focused either on the extraction of high value-added compounds or on the fractionation of the lignocellulosic material. Therefore, in the first instance, three classes of DESs based on choline chloride as HBA were tested for their ability to extract polyphenols from CSW at low temperatures. Then, the biorefining of the solid residue was explored by attempting a separation of lignin and cellulose using a bio-IL (Figure 1). The three parallel reaction model combined with the distributed activation energy model (DAEM) was used to predict the composition of the pristine CSW and of the fractions obtained after the DES and bio-IL treatments. Recycling tests of the best performing DES and recovery of the bio-IL were also carried

Table 1. DES Molar Ratio and Preparation Conditions

Name	HBA	HBD	Molar ratio	T (°C)
ChCl:EG (Choline Chloride-ethylene glycol)			1:4	25
ChCl:But (Choline Chloride-1,4-butanediol)			1:4	25
ChCl:Oax2H$_2$O (Choline Chloride-oxalic acid dihydrate)			1:1	40
ChCl:Ma (Choline Chloride-malic acid)			1:1	80
ChCl:CaxH$_2$O (Choline Chloride-citric acid hydrate)			1:1	80
ChCl:Mal (Choline Chloride-maltose)			1:1	80
ChCl:Glu (Choline Chloride-glucose)			1:1	80
			1:2	80

out to get further information on the feasibility of the proposed process.

MATERIALS AND METHODS

Choline chloride (ChCl), oxalic acid dihydrate (Oax2H$_2$O), malic acid (Ma), and ethylene glycol (EG) were purchased from Alfa Aesar (Thermo Fisher Scientific). Cholinium hydroxide in methanolic solution 45%, citric acid hydrate (CaxH$_2$O), 1,4-butane diol (But), maltose (Mal), glucose (Glu), glycine, gallic acid, catechin hydrate, procyanidin B2, vanillic acid, (−) epicatechin, syringic acid, p-coumaric acid, $trans$-ferulic acid, propyl gallate, ellagic acid hydrate, 3,5-di-$tert$-butyl-4-hydroxybenzaldehyde, ethoxyquin, quercetin, nor-dihydroguaiaretic acid, 3-$tert$-butyl-4-hydroxyanisole, 2,6-di-$tert$-butyl-4-hydroxymethyl phenol, octyl gallate, lauryl gallate, tert-butylhy-droquinone, methanol, and Amberlite XAD-7 were purchased from Sigma-Aldrich (Merck Life Science). The CSW was provided by "Ortofrutticola Del Mugello s.r.l."; it was ground and dried at 60 °C in an oven for 16 h before use.

Preparation of DESs. Prior to the synthesis, ChCl was dried under vacuum for 6 h at 80 °C. Briefly, ChCl and the corresponding HBD (carboxylic acid, polyol, or sugar) were mixed in an appropriate molar ratio until a homogenous transparent liquid was formed; see Table 1. The carboxylic acid-based DESs (except for ChCl:Oax2-H$_2$O) and the sugar-based DESs were prepared at 80 °C. Polyol-based DESs were prepared at room temperature, while ChCl:Oax2-H$_2$O DES was prepared at 40 °C. After the DES formation, no purification step was needed and the DESs were kept at room temperature in sealed vessels until their use. The DESs with malic acid and sugars as HBD were mixed with 25 wt % of water in order to reduce their viscosity.[35,36] ^{1}H NMR spectra (D$_2$O) of DESs are shown in Supporting Information (Figures S4−S11).

Synthesis of the Ionic Liquid (Cholinium Glycinate). Prior to use, commercial choline hydroxide (ChOH) methanolic solution (ca. 45%) was titrated with 1 M HCl giving the exact percent of ionic liquid in MeOH (44.3%). A slight excess (1.2 mol) of aqueous solution of glycine was added dropwise to the ChOH solution at 0 °C, and the mixture was stirred overnight. Then, methanol was removed under reduced pressure. A mixture of acetonitrile/methanol (9/1 v/v) was added under vigorous stirring to precipitate the excess of amino acid, which was then filtered off. The filtrate was evaporated to remove solvents at 50 °C, and the obtained IL was dried in vacuo for 24 h using the same temperature.[37] The correct stoichiometry was verified by means of the ^{1}H NMR spectrum registered in D$_2$O (Figure S12, see Supporting Information).

Extraction of Polyphenols. Polyphenol extraction from CSW was performed in glass reactor tubes with PTFE caps. The solid to solvent ratio was fixed at 1/10 (w/w), 5 g of DES, and 0.5 g of CSW.[38] Then, the mixture was extracted under fixed conditions of temperature (65 °C) and time (24 h), under magnetic stirring. After 24 h, the mixture was cooled down to room temperature, diluted with MeOH/H$_2$O (70/30), and filtered (sintered filter) until a clear solution came out. The undissolved solid residue was collected with a

spatula and was dried in an oven at 65 °C. The supernatant was collected and concentrated under reduced pressure to recover the MeOH used during the washing. After this, the polymeric resin, Amberlite XAD-7 (50 g), was used to separate the phenolic compounds from the recovered water DES phase.[39] Prior to use, the resin was washed and activated by stirring it with acidified water (0.01 M HCl) for 30 min. The activated resin was put into a column and the filtrate was added. The DES was removed washing with water and the absorbed polyphenol-polymeric resin was washed with water until it reaches neutral pH. Subsequently, the absorbed polyphenol-polymeric resin was dried with an airflow and the extracted polyphenols were desorbed from the resin with MeOH (~150 mL). Following that, the methanolic extract was evaporated under reduced pressure for recovering the polyphenolic extracts. The yields of recovered polyphenols are reported in Table S1 (see Supporting Information). Then, the extracts were dissolved in 10 mL of MeOH and the total polyphenol content and total condensed tannins were quantified with colorimetric assays. HPLC analyses were performed for the identification and quantification of polyphenols. The extraction efficacy of the studied DESs was compared with a classical extraction of MeOH/H$_2$O (70/30 v/v), which was performed keeping unchanged all the parameters used in the extraction of polyphenols with DES.

Recovery and Reuse of ChCl:Oax2H$_2$O. The recovery and the reuse of the solvent were evaluated for the best performing system studied (ChCl:Oax2H$_2$O) for the extraction of polyphenols. More in detail, the aqueous fraction obtained washing the polymeric resin was evaporated under reduced pressure for recovering the DES. Subsequently, the recovered DES was reused without any modification for a new extraction process with fresh biomass waste as described in the previous section. The solvent was recycled three times and analyzed by ^{1}H NMR in D$_2$O (Figure S13). The extraction efficiency of the recovered DES was evaluated through the determination of the total phenolic content (TPC) of the methanolic extracts (as reported in the next section).

Determination of TPC of the Extract. Total polyphenolic content was determined spectrophotometrically according to the Folin−Ciocalteu procedure as described by Rodrigues et al.[40] Briefly, 500 μL of the sample methanolic solution was mixed with 2.5 mL of the Folin−Ciocalteu reagent (10× dilution) and a transparent yellow solution appeared. After 5 min, 2.5 mL of the 7.5% aqueous solution of Na$_2$CO$_3$ was added. The flasks were kept in a water bath at 45 °C for 15 min. The initial yellow color of the samples changed into blue and the absorbance was measured at 765 nm. Gallic acid was employed to prepare the calibration curve ($y = 0.0097x − 0.0039$; $R^2 = 0.99847$), and the results were expressed in mg of gallic acid equivalents (GAEs) per g of dry biomass.

Vanillin-HCl Assay. The vanillin-HCl assay was performed for the quantification of condensed tannins (proanthocyanidins) in the extracts. This colorimetric assay, in contrast with the Folin−Ciocalteu assay, is specific for a narrow range of polyphenols; that is, the flavanols that have a single bond at the 2,3 position and free m-oriented hydroxyl groups on the B ring.[41] Briefly, 1 mL of the sample solution was mixed with 2.5 mL of the 1% vanillin solution in MeOH. Subsequently, 2.5 mL of the 9 M HCl solution was added and the mixture was incubated at 30 °C for 20 min. In addition, a control sample was used in which vanillin was replaced with MeOH. Finally, the absorbance was measured at 500 nm. For each sample solution, we calculated A by eq 1 as

$$A = (A_s − A_b) − (A_c − A_0) \tag{1}$$

where: A_0 = 1 mL of methanol + 2.5 mL of 9 M HCl, A_b = 1 mL of methanol + 2.5 mL of 1% vanillin solution + 2.5 mL of 9 M HCl, A_c = 1 mL of sample solution + 2.5 mL of methanol + 2.5 mL of 9 M HCl, and A_s = 1 mL of sample solution + 2.5 mL of 1% vanillin solution + 2.5 mL of 9 M HCl.

Prior to this, catechin hydrate (0−400 μg/mL in methanol) was used to prepare the calibration curve ($y = 0.00197x$; $R^2 = 0.99824$). The results were expressed as mg of catechin hydrate equivalents per

g of dry biomass. For each sample, the vanillin-HCl assay was performed three times.

HPLC Analysis. The separation and identification of polyphenols from CSW was performed using a C18 Shimadzu column (150 mm × 46 mm × 4.5 μm) on a Shimadzu LC 20 with DAD detector.

The mobile phases were 0.2% (v/v) formic acid-water (eluent A) and MeOH (eluent B). The flow rate was 1 mL/min, the injection volume was 20 μL, and the column temperature was set to 40 °C. Gradient elution was performed as follows: 0−5 min, 5% B; 5−55 min, linear gradient up to 95% B; 55−65 min, 95% B; and 65−67 min, linear gradient up to 5% B. Postrun time was 15 min. Gallic acid, catechin hydrate, procyanidin B2, vanillic acid, (−) epicatechin, syringic acid, p-coumaric acid, trans-ferulic acid, propyl gallate, ellagic acid hydrate, 3,5-di-tert-butyl-4-hydroxybenzaldehyde, ethoxyquin, quercetin, nordihydroguaiaretic acid, 3-tert-butyl-4-hydroxyanisole, 2,6-di-tert-butyl-4-hydroxymethyl phenol, octyl gallate, lauryl gallate, and tert-butylhydroquinone were used as analytical standards for HPLC quantification. The chromatographic peaks of analytes were confirmed by comparing their retention times and UV spectra with those of the reference compounds. Figure S14 (see Supporting Information) shows the HPLC chromatograms of the standards.

Fractionation of Lignocellulosic Residue and Recovery of the IL. After the extraction of polyphenols, the undissolved residue was dried at 65 °C in an oven. Subsequently, this was treated with cholinium glycinate (ChGly) as described previously by An et al. 2015, with minor modifications.[34] Briefly, the biomass was treated with the IL at 90 °C for 16 h with a biomass/IL ratio of 1/20 (w/w). Then, the mixture was diluted with a NaOH solution (0.1 M). The solid fraction (cellulose-rich material, CRM) was recovered by filtration and washed with the same basic solution. At this point, the filtrate was acidified to pH 2 with HCl (4 and 1 M) to precipitate the lignin. The recovered lignin-rich material (LRM) was washed with acid water. The two fractions were then dried at 70 °C in an oven for 72 h prior to the characterization. After the recovery of the LRM, the acidified filtrate was basified to pH 11.5 (the pH of the aqueous solution of the IL) with NaOH (4 and 1 M). Water was removed by evaporation under reduce pressure. Anhydrous MeOH was added to the residue, leaving NaCl as the insoluble solid, which was removed by filtration. MeOH was evaporated under reduced pressure and the recovered IL was analyzed by ^{1}H NMR spectroscopy (Figure S15).

Determination of the Solvatochromic Parameters (π^* and α) of the DESs. The solvatochromic probes N,N-diethyl-4-nitroaniline (NEt$_2$) and Nile Red (NR) were used to determine the dipolarity/polarizability (π^*) and the hydrogen-bond acidity (α) of all the tested DESs. Nile Red was selected in place of the Reichardt'dye 30 on account of the quite sensitivity to acids of this latter dye.[42] Reichardt' dye 33 was also tested, but it was not soluble in the acid-based DESs and was discarded.

For the analysis, a proper amount of the dyes was dissolved in the different solvents. It is to note that in the case of DESs containing malic acid and sugars as HBDs, 25 wt % of water was added. Subsequently, the absorbance was measured with an UV−vis spectrophotometer at room temperature and at 65 °C.

The solvatochromic parameters were determined using the following equations

$$\pi^* = 0.314\, x(27.52 − \nu_{NEt2}) \tag{2}$$

$$\alpha = \frac{(19.9657 − 1.0241\pi^* − \nu_{NR})}{1.6078} \tag{3}$$

$$\nu = \frac{10^4}{\lambda_{maxprobe}} \tag{4}$$

where, ν and $\lambda_{maxprobe}$ are the experimental wave number and the maximum wavelength of the probes.

Fourier Transform Infrared Spectroscopy. The ATR-Fourier transform infrared spectroscopy (FTIR) spectra were recorded with an Agilent Technologies IR Cary 660 FTIR spectrophotometer using a macro-ATR accessory, a Diamond crystal. The spectra were
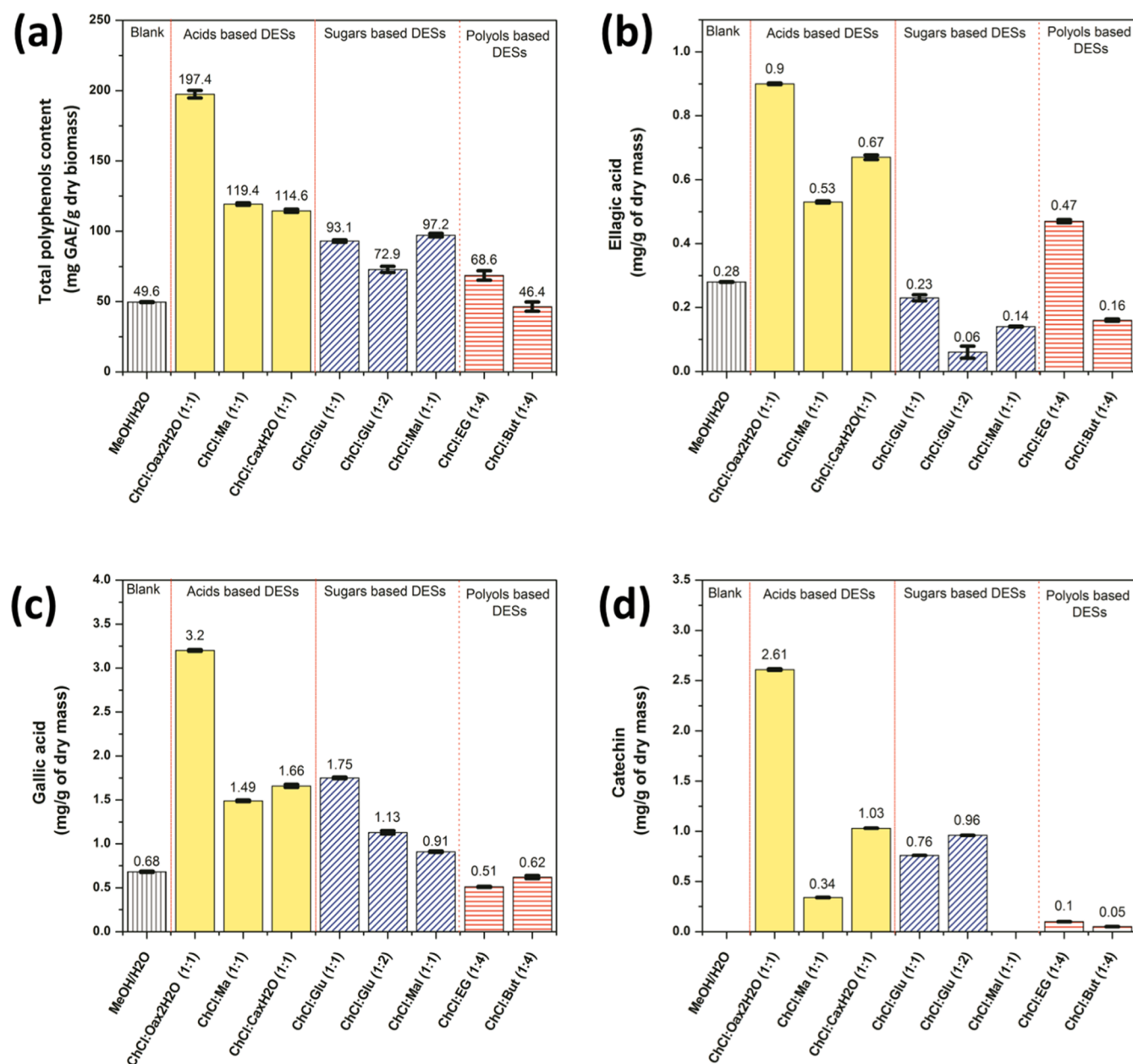
Figure 2. (a) Total polyphenol content (TPC) obtained from the Folin−Ciocalteu assay, and HPLC quantification for (b) ellagic acid, (c) gallic acid, and (d) catechin.

measured in the range from 4000 to 500 cm^{-1} with 32 scans. The moisture and CO_2 were eliminated from the samples by measuring first the background spectra before each sample.

Ultraviolet−Visible Spectroscopy. The Folin−Ciocalteu assay and the vanillin-HCl assay were performed with an Agilent Cary 300 UV−vis spectrophotometer at working wavelengths of 765 and 500 nm, respectively.

Nuclear Magnetic Resonance Spectroscopy. ^1H NMR spectra were recorded with a Bruker AVANCE II spectrometer operating at 400 MHz. The samples were prepared in 5 mm tubes using D_2O. The chemical shift (δ) was referenced to the chemical shift of D_2O (δ_H 4.79).

Thermogravimetric Analysis. Thermogravimetric curves were registered with a TGAQ500 (TA instruments) at a heating rate of 10 °C/min, from 30 to 800 °C under N_2 flow.

Nonlinear Least Square Fitting of Three Parallel Model. Calculation Details. The first order three parallel reaction model combined with the distributed activation energy model (DAEM) is described using eq 5.[43−45]

$$m = m_{\text{final}} + \sum_{i=1}^{3} c_i(1 - m_{\text{final}})\left\{\frac{1}{\sigma_i\sqrt{2\pi}}\int_0^\infty \exp\left[-\frac{(E - E_{i,0})}{2\sigma_i^2}\right.\right.$$
$$\left.\left. - \frac{A_i}{\beta}\int_{T_0}^T \exp\left(-\frac{E}{RT}\right)dT\right]dE\right\} \quad (5)$$

where m = instantaneous mass and m_{final} = final mass of the pyrolytic process, T = temperature (K), c_i = fraction of volatiles produced, A_i = pre-exponential factor (s^{-1}), β = heating rate (K/s), E = activation energy (kJ/mol), $R = 8.314 \times 10^{-3}$ universal constant (kJ/mol K), $E_{i,0}$ = mean activation energy (kJ/mol), and σ_i = standard deviation (kJ/mol) of $E_{i,0}$. The subscript $i = 1......3$ refers to the ith component (1 = hemicellulose, 2 = cellulose, and 3 = lignin).

Equation 5 was solved by numerical calculation for each experimental data allowing to fit the full set of experimental points ($N \approx 4700-5200$ points) by coding in Matlab. The variables (A_i, E_i, σ_i, c_i) were determined using stochastic global optimization

(Simulated Annealing Algorithm) by minimizing the objective function

$$\min_{(A_i, E_i, \sigma_i, c_i)} \sum_{i=1}^{N} (m_{obs} - m_{calc})^2 \qquad (6)$$

All the data were calculated numerically without any approximation for the Arrhenius function (dT integration).

The fitting quality (eq 7) was calculated using the final value of the objective function (O.F. = final value of eq 6), the total number of evaluation points, and the maximum value of mass as

$$\text{fit}(\%) = 100 \cdot \frac{\left(\frac{\text{O.F.}}{N}\right)^{1/2}}{m_{max}} \qquad (7)$$

The TG experimental data used to fit the three parallel-DAEM model were firstly identified through the second derivative method.[44] Figure S16 (see Supporting Information) shows the second derivative of TG curves (DDTG) for CSW, CSWR, CRM, and LRM. The lignocellulosic pyrolysis process was then divided into three steps using the corresponding local minimum of the DDTG curve. The full set of characteristic temperature values and initial and final masses for all the samples are listed in Table S2 (see Supporting Information). The limits of dE integration were from 0 to $E_0 + 30\sigma_i$ according to Cai et al.[45]

■ RESULTS AND DISCUSSION

Extraction of Polyphenols. The physical and chemical properties of DESs are influenced by their structure. In the present study, three classes of choline chloride (ChCl)-based DESs, characterized by different HBDs such as polyols, acids, and sugars, were selected for the polyphenol extraction. When malic acid, glucose, and maltose were used as HBDs, the respective DESs appeared too viscous at the operative temperature and hence 25 wt % of water was added. Several research groups have investigated the influence of water on DES properties.[46−48] For the systems studied here, it is already known that the addition of water leads to a decrease in viscosity.[49] It has been reported that the viscosity of DESs hinders the extraction of biologically active compounds such as polyphenols because of the low mass transport efficiency.[50] Bubalo et al. used various DESs based on sugars or acids and found that 25 wt % of water improved the anthocyanin extraction from grape skin pomaces.[36] The same amount of water (25 wt %) had a beneficial effect when polyphenols were extracted from *Aegle marmelos* with the ChCl:oxalic acid (1:1) DES.[48]

A classical extraction with a methanol/water (70/30) solution using a biomass/extractant solvent ratio of 1/10 (w/w) at 65 °C for 24 h was performed.[38] Indeed, this reference extraction result is needed as literature comparisons are often inconclusive, as already observed by Vella et al.[51] because of the different experimental conditions employed for the extraction of polyphenols from CSW or because of the different starting biomass sources. More specifically, the waste can be of outer shell or inner shell origin as well as mixed; alternatively, CSW can in some cases undergo pretreatments like "brulage" or boiling.

The DESs were subsequently screened for their polyphenol extraction efficiency under the same conditions. After the extraction, an adsorbent polymeric resin, Amberlite XAD-7, was used for the separation of the DESs from the extract. Indeed, the resin adsorbs the phenolic compounds while the polar components of DESs are eluted with water. The phenolic compounds were desorbed from the resin with the minimum

amount of methanol. The total polyphenolic content of the extract was quantified with the aid of the Folin−Ciocalteu assay. The results are shown in Figure 2a. A value of 49.6 mg/g of GAE was obtained with the classical extraction (labeled as MeOH/H$_2$O in Figure 2). A comparable value was achieved with ChCl:But (1:4) (46.4 mg/g of GAE) followed by the other polyol-based DES [68.6 mg/g of GAE for ChCl:EG (1:4)]. The value of TPC increased to 93.1 and 97.2 mg/g of GAE for ChCl:Glu (1:1) and ChCl:Mal (1:1), respectively, while over 100 mg/g of GAE was registered when acid-based DESs were employed. Among them, the highest capacity for polyphenol extraction was achieved using the ChCl:Oax2H$_2$O DES (197.4 mg/g of GAE).

Based on these results, ChCl:Oax2H$_2$O was the best performing system for polyphenol extraction and it was further tested in the attempt to understand the effect of experimental conditions on the extraction efficiency. At first, temperature and the solid to DES ratio (1/10) were kept unchanged while the extraction time was reduced from 24 h to 12 and 6 h, and the total polyphenol content was measured. A decrease in the TPC value was observed (159.6 mg/g of GAE for 12 h and 121.2 mg/g of GAE for 6 h). Because the highest value for TPC was registered at 24 h, the experiment was repeated changing only the operative temperature from 65 °C to room temperature. The Folin−Ciocalteu assay was performed and a value of 107.7 mg/g of GAE, lower with respect to that achieved at higher temperature, was registered.

The use of DESs in extractions represents a substantial improvement when compared to the classical method, thus implying a better affinity of these media with the phenolic compounds. The high TPC values obtained with acid-based DESs could be ascribable also to the partial depolymerization of lignin present in the pristine chestnut shell. Indeed, lignin is a polyphenolic material characterized by strong intra and intermolecular hydrogen bonds and π−π stacking interactions between its aromatic rings. Acid-based DESs such as ChCl:lactic acid, ChCl:oxalic acid, or ChCl:p-toluenesulfonic acid were used for the extraction of lignin. However, a depolymerization process was also observed, which caused the fractionation of lignin into lower molecular weight phenolic compounds.[52,53] Attempts to explain the mechanism of dissolution of lignin-carbohydrate complexes with DESs were made by Liu et al.[54] Very recently da Costa Lopes et al. showed that acidic DESs play an important role in biomass delignification. They used a lignin model (2-phenoxy-1-phenylethanol) and demonstrated that besides the acidic nature of each DES, the halide anion (Cl- or Br-) portion contributes to lignin processing by cleaving the β-O-4- ether bonds of the compound.[55] Recent studies described further lignin modifications when DESs based on choline chloride and oxalic acid or lactic were used for its dissolution.[52,53,56−59]

To gain insight into the different extraction performances of the three DES classes characterized either by acid, sugar, or alcohol HBDs, the π* and α Kamlet−Taft parameters of all the tested DESs were measured, both at room temperature and at the working extraction temperature of 65 °C (Table 2). In the case of DESs containing malic acid and sugars as HBDs, 25 wt % of water was added as for the extraction process.

The π* and α parameters quantify the polarity/polarizability and the hydrogen-bond donating ability of the solvents, respectively. It is of note that temperature plays a minor role in both parameters, which is in agreement with previous findings.[60] Only the α parameter for the glucose-containing

Table 2. Solvatochromic Parameters π^* and α of the Used DESs at 25 and 65 °C

DES composition	mol ratio (ChCl:HBD)	Kamlet−Taft parameters (25 °C)		Kamlet−Taft parameters (65 °C)	
		π^*	α	π^*	α
ChCl:Oax2H$_2$O	1:1	1.21	1.23	1.19	1.28
ChCl:Ma[a]	1:1	1.28	1.18	1.24	1.21
ChCl:CaxH$_2$O	1:1	1.24	1.22	1.23	1.24
ChCl:Mal[a]	1:1	1.35	0.94	1.35	0.90
ChCl:Glu[a]	1:1	1.31	0.98	1.31	0.88
ChCl:Glu[a]	1:2	1.32	1.05	1.32	0.89
ChCl:EG	1:4	1.13	0.77	1.10	0.75
ChCl:But	1:4	1.05	0.68	1.03	0.67

[a]25 wt % of water was added to the DES.

DESs decreases significantly at 65 °C. The α Kamlet−Taft parameter values for the different HBDs (acids > sugars > alcohols) correlate well with the extraction efficiency picture reported in Figure 2a. This scenario suggests that higher α parameters allow for a stronger interaction between the biomass and the DES, a behavior that has been reported before in lignin fractionation studies.[61,62] In particular, the ChCl-glycerol DES, characterized by an α of 0.77, was unable to fractionate the biomass studied.[62]

The extraction results for the individual polyphenols, discussed in the following section (Figure 2b−d), call for the presence of subtle interactions between the polyphenol and the partner DES system and demand further investigations, which will be the subject of a forthcoming study.

The total polyphenol content test is a general test for the detection of polyphenols, but it does not give qualitative information about the actual molecules that are present in the extracts. HPLC analyses were performed for the identification of the polyphenols contained in the extracted mixtures. Figure 3 shows representative chromatograms (absorbance at 280 nm) for the extracts obtained using the different classes of DESs: ChCl:Oax2H$_2$O, ChCl:Glu (1:1) and ChCl:EG (1:4). Figures S17−S20 show the corresponding chromatograms for
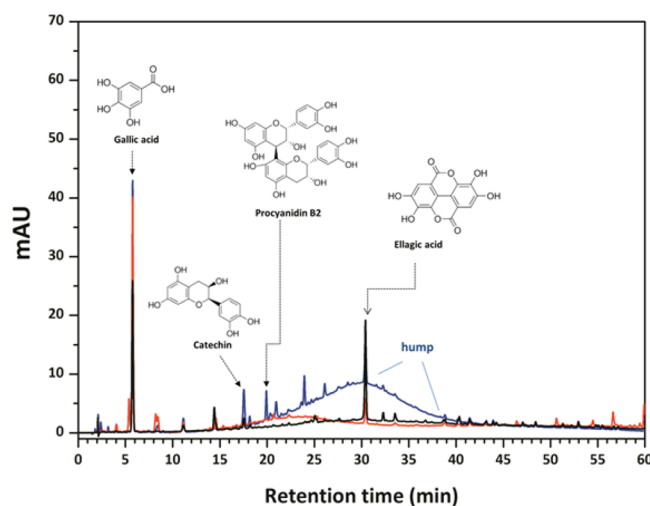

Figure 3. HPLC chromatograms of extracts with different DESs at 280 nm: (a) ChCl:Oax2H$_2$O (1:1) (blue curve), (b) ChCl: Glu (1:1) (red curve), and (c) ChCl: EG (1:4) (black curve).

the extracts obtained using ChCl:Ma (1:1), ChCl:But (1:4), ChCl:Glu (1:2), and ChCl:Mal (1:1), respectively. The concentration of the samples was 800 μg/mL and the same mobile phase was used in the preparation of both the samples and of the standards. For gallic acid, ellagic acid, procyanidin B2, vanillic acid, and catechin, calibration curves were constructed and the content of these compounds in real samples was measured. The ability of DESs to extract polyphenols varied considerably from one DES to another. The chromatograms in Figures 3 and S17−20 (see Supporting Information) show three major peaks present in all samples: gallic acid (rt 5.7 min), catechin (rt 17.6 min), and ellagic acid (rt 30.4 min). This behavior is in perfect agreement with the major phenolic components identified in the literature for the same biomass.[63] Again, in accordance with the results obtained with the Folin−Ciocalteu assay, ChCl:Oax2H$_2$O extracted the highest amount of these polyphenols (3.20 mg/g of gallic acid, 2.61 mg/g of catechin, and 0.90 mg/g of ellagic acid, see Figure 2b−d). Moreover, only in the extract obtained with ChCl:Oax2H$_2$O, we were also able to detect and quantify vanillic acid (0.27 mg/g of dry mass) and procyanidin B2 (0.98 mg/g of dry mass). Finally, ChCl:Oax2H$_2$O extracted 4-fold more gallic acid and ellagic acid than the MeOH/H$_2$O system (as it is shown in Figure 2b,c respectively), while catechin was not detected in the methanolic extraction (see Figure 2d).

It is worth mentioning that the color of the extracts varied when different DES classes were employed (Figure S21, see Supporting Information). This phenomenon could indicate a different composition of the extract, as some phenolic compounds such as anthocyanins or condensed tannins are deeply colored species. More specifically, the polyphenols extracted with ChCl:Oax2H$_2$O had a purple color, those recovered with acid-based DESs were red, whereas those obtained with sugar-based DESs were orange. In contrast, pale yellow extracts were afforded when polyol-based DESs were used. The high capacity of acid-based DESs such as ChCl:Oax in the extraction of polyphenols such as anthocyanins from grape skin was reported by Bubalo et al.[36] They assumed that an important factor in the extraction of these components is the DES polarity that varied in the following order acids > sugar > polyols.[35,36,64]

Furthermore, in the chromatograms shown in Figure 3, a large and intense hump can be noticed in the case of the extracts obtained with ChCl:Oax2H$_2$O DES. This hump diminishes when employing DES of different nature, from acid ones to sugar-based ones (ChCl:Glu), while it is negligible in the case of polyol-based DESs.

It has been reported before that an unresolved large peak in the chromatogram could be attributed to condensed tannins present in the sample.[5] Based on the different colors of the extracts (Figure S21) as well as on the different intensity of the unresolved large peak obtained in the chromatograms (Figure 3), the vanillin-HCl assay was performed to confirm the presence and quantify the condensed tannins contained in the extracts (Figure 4). Indeed, the highest content was registered for the ChCl:Oax2H$_2$O system (189.6 mg CE/g dry chestnuts) followed by the other two acid-based DESs.

Conversely, the test was negative for the extracts obtained with polyol-based DESs, which did not show the hump in their chromatograms. Sugar-based DESs presented instead values between 12 and 50 mg CE/g dry. These data suggest, therefore, that condensed tannins are the main class of polyphenols present in the extracts. Our findings are in good
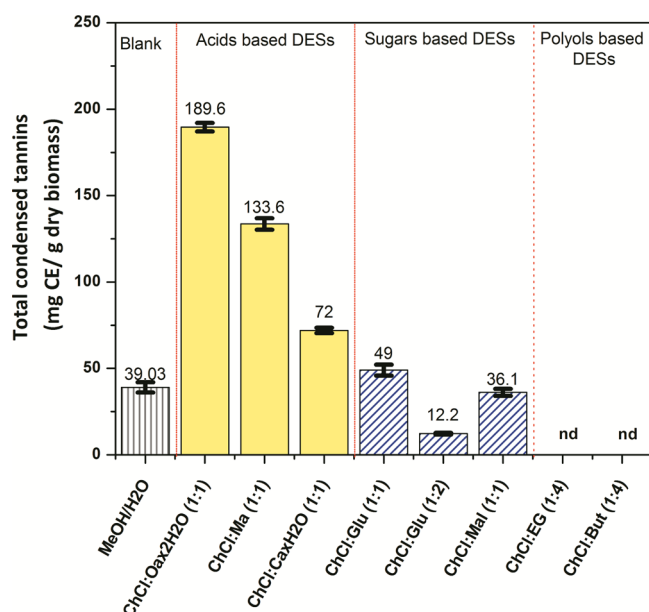
Figure 4. Total condensed tannin content of the extracts with different DESs.

Figure 5. Yield of the recovered DES and extraction efficiency after each cycle.

agreement with the work of Squillaci et al. who found that up to 25 mg/g of the 43.6 mg/g of GAE total polyphenolic content in their extracts were condensed tannins.[63] These results confirm the possibility of modulating the polyphenol extraction efficacy by changing the HBD component of the DES involved in the CSW processing. Cao et al. reported the high capacity of ChCl:malonic acid with 55 wt % of water in the extraction of proanthocyanidins (condensed tannins) from Gingko biloba leaves. The authors also noticed that the acid-based extract had a dark red color, while those obtained with classical organic solvents such as methanol or ethanol had a yellow-brown tinge because of the different types of proanthocyanidins extracted.[65]

Recovery and Reuse of ChCl:Oax2H₂O. The recovery of the solvent from an extraction process, the following use in a new extraction cycle, and the retention of its extraction efficiency (EE) are all aspects, which concur to define the real sustainability of a process. Therefore, our best performing DES (ChCl:Oax2H₂O) was tested in four consecutive extraction cycles and the results obtained are summarized in Figure 5. The DES recovery is reported as the percentage of mass recovered over mass used, while the extraction efficiency was assessed on the basis of the TPC of the methanolic extracts after each extraction cycle.

As previously reported,[19] the DES can be recovered from the filtrate aqueous solution by removing water by heating under reduced pressure, after filtration through the Amberlite XAD-7 resin (please refer to the Materials and Methods section). ¹H NMR analysis showed that the DES was obtained in high purity after each cycle, presenting the known[66] ester side product, which derives from the reaction between the HBA and the HBD, as the sole recognizable contaminant (Figure S13).

A slight decrease in the recovery yield and in the extraction efficiency was observed until the third cycle, after which a stabilization of both parameters was noticeable. This outcome could be, at least in part, ascribable to the increasing formation of the ester side product up to a certain extent. The ¹H NMR spectral comparison seems to corroborate this hypothesis as its
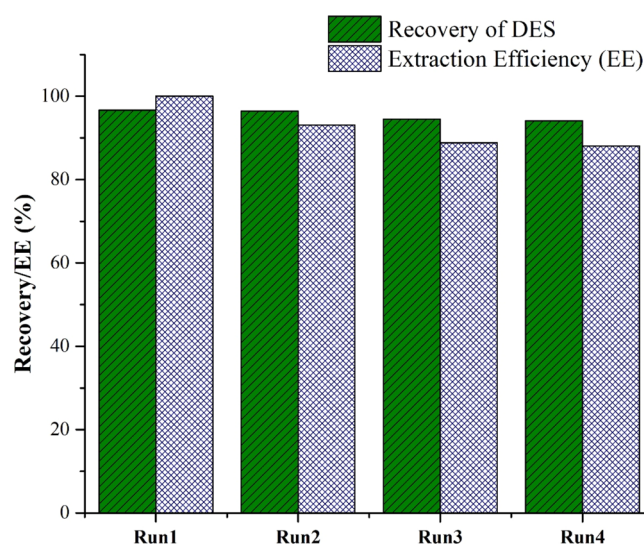
content increases up to 10%, albeit only in the first three cycles (Figure S13). Overall, this DES appears to be a good candidate for large scale studies, where it can be anticipated that additional optimization has the potential to further minimize the formation of the detrimental ester side product.

Fractioning of Lignocellulosic Residue. Lignin is one of the most recalcitrant natural polymeric compounds. In the lignocellulosic material, lignin holds cellulosic fibers together and acts as a bonding and stiffening agent. In biorefineries, delignification pretreatments or fractionation processes of lignocellulosic materials represent a key step for the production of biofuels and added value chemicals. Among the cholinium-amino acids ILs, ChGly showed the highest lignin dissolution power and a negligible ability to dissolve xylan and cellulose.[67] Thanks to these peculiar properties, this IL was employed for the delignification of rice straw before enzymatic hydrolysis experiments and for the fractionation of different hard and softwoods biomasses.[34]

Therefore, this bio-based and nontoxic IL was selected to complete the valorization of the CSW. After the separation of the polyphenols with ChCl:Oax2H₂O, the chestnut shell residue (henceforth labeled CSWR) was first dried in an oven at 65 °C and then treated with ChGly (see Figure 1). Following the procedure developed by An et al.,[34] after treatment with the bio-IL (5% biomass loading, for 16 h at 90 °C), a solution of NaOH (0.1 M) was added and the undissolved residue enriched in cellulose (CRM) was filtered away. The collected filtrate was acidified to precipitate the dissolved lignin. The precipitate enriched in lignin (LRM) was recovered by centrifugation and washed with acidic water. After the precipitation of lignin, further treatments of the acidic centrifuged solution were required for the recovering of the IL: (1) adjustment of the pH to that of an aqueous solution of ChGly by adding aqueous NaOH (1 and 4 M), (2) removal of the water under reduced pressure, (3) dissolution of the IL in dry methanol and filtration of the undissolved salts, and (4) removal of the methanol under reduced pressure. ChGly was recovered in both satisfactory amounts (>97%) and purity (please refer to the ¹H NMR comparison reported in Figure S15). The CRM and LRM fractions were dried in an oven at 65 °C and were recovered in amounts equal to 54 and 8% of

the CSWR, respectively. FTIR analysis was performed to characterize the two materials and to compare them with the FTIR spectrum of CSWR (Figure 6). The spectrum of this
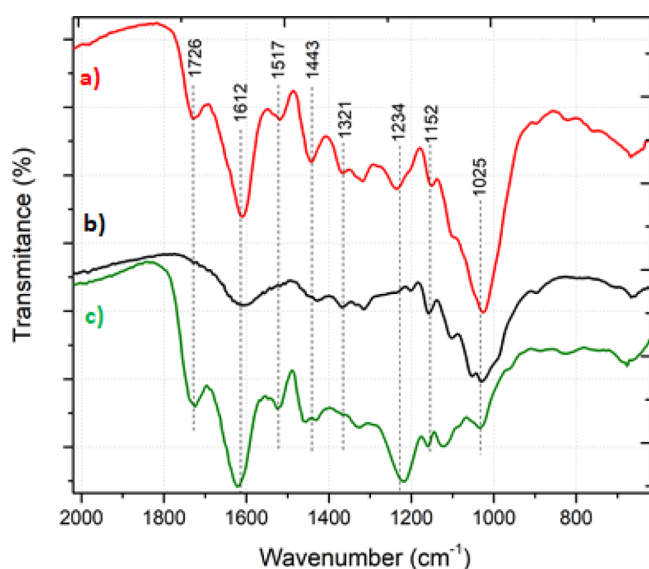

Figure 6. FTIR spectrum of (a) CSWR, (b) CRM, and (c) LRM extracted with ChGly.

latter residue displays all the characteristic bands attributable to the three main components of lignocellulosic materials. Indeed, the band at 1726 cm^{-1} corresponds to the C=O stretching mode of ester groups such as acetyl, feruloyl, or p-coumaroyl groups found in hemicellulose and lignin,[68] the bands at 1517 and at 1443 cm^{-1} were characteristic of the C=C stretching vibrations of the phenol rings and of the deformation mode of aromatic rings that are present in the structure of lignin. The intense vibrational band between 1100 and 900 cm^{-1} with the maximum at 1025 cm^{-1} is instead a distinctive feature of the vibrational modes of cellulose/hemicellulose glycosidic linkages. The FTIR spectrum of Figure 6b represents the CRM obtained after the treatment with ChGly. It can be observed that the characteristic peaks of lignin disappeared, while the intense distinguishing absorption peaks of the C−O−C vibration modes at 1025 and 1045 cm^{-1}

of cellulose are still present. In the FTIR spectrum of LRM (Figure 6c), a lowering of the intensity of the peak between 1100 and 900 cm^{-1}, characteristic for cellulose, can be noticed. Diagnostic bands of lignin are present in this spectrum with the maximum peaks at 1726, 1517, and 1234 cm^{-1}. This clearly shows the successful separation of lignin.

The thermal degradation of the obtained fractions was investigated; TG and DTG curves obtained under an inert atmosphere (N$_2$) from CRM, LRM, and CSWR samples are reported in Figure 7a,b, respectively. CSW was also analyzed for the sake of comparison.

As reported in the literature, four major steps can typically be identified during the pyrolysis of a lignocellulosic biomass: (I) moisture evaporation below 150 °C, (II) mass loss related to the hemicellulose portion in the temperature range of 150−300 °C, (III) mass loss of the cellulose portion in the temperature range of 300−400 °C, and (IV) lignin decomposition in the temperature range of 150−900 °C.[69−72] As shown in Figure 7, the thermogravimetric curves for CSW, CSWR, and CRM presented similar profiles and displayed all the expected degradation steps of lignocellulosic biomass. In particular, the DTG curves (Figure 7b) are characterized by a main sharp peak (because of cellulose decomposition) partially overlapped with a shoulder peak at a lower temperature (because of hemicellulose decomposition) and a long tail observed at a higher temperature (because of lignin decomposition). Different T_{peak} and different distributions of the three main degradation steps were observed because of the heterogeneous nature and different compositions of the biomass samples. Table 3 summarizes the thermal degradation steps (identified as T_{peak} from the DTG curves, Figure 7b) and the corresponding mass losses observed for CSW, CSWR, and CRM. It is worth stressing again that the degradation of lignin occurs in a wide temperature range, which clearly limits the direct correlation of mass loss composition.

LRM showed a completely unique thermal decomposition behavior and its thermogravimetric profile was very similar to those reported by Manara et al. for lignins extracted from a different agricultural waste. The thermal behavior of LRMs depends on the extraction method as well as on the type of biomass. Indeed, they studied the extraction of lignin with different processes from various types of agro-wastes and they
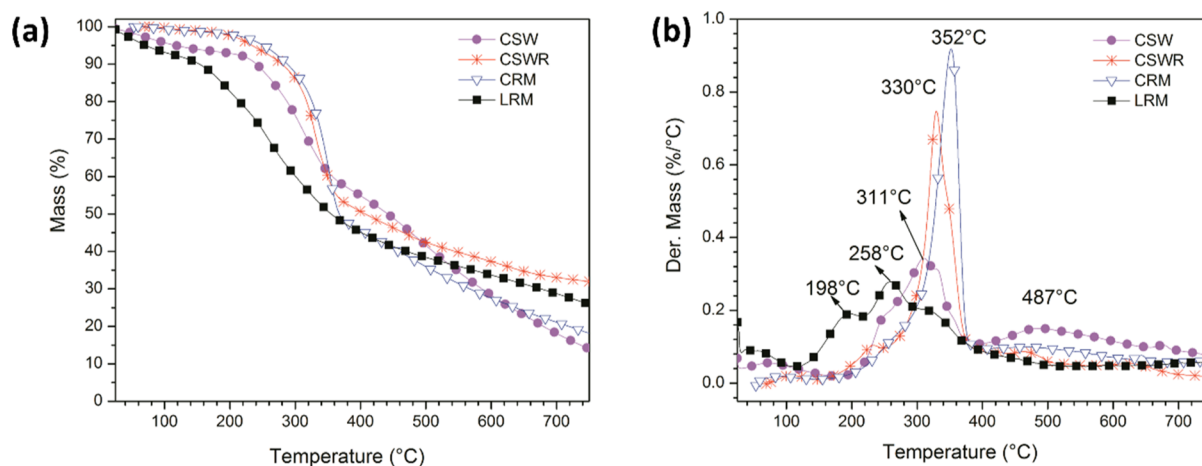

Figure 7. TG (a) and DTG (b) curves for pristine CSW, residue after polyphenol extraction with ChCl:Oax2H$_2$O (1:1) (CSWR), CRM after treatment with ChGly (CRM), and LRM extracted with ChGly (LRM).

Table 3. Steps of Degradation for CSW, CSWR, CRM, and LRM

samples	mass losses (%)				
	step I (<150 °C)	step II (150–300 °C)	step III (250–400 °C)	step IV (400–750 °C)	residue at 750 °C (%)
CSW	6.1 (77 °C)	7.6 (249 °C)	31.4 (311 °C)	40.8 (487 °C)	14.1
CSWR	1.1 (107 °C)	5.5 (230 °C)	42.7 (330 °C)	18.6 (467 °C)	32.1
CRM	1.3 (91 °C)	7.6 (279 °C)	45.4 (352 °C)	27.5[a]	18.2
LRM	7.8 (62 °C)	12.6 (198 °C)			
		20.3 (258 °C)	14.2 (315 °C)	19.3[a]	25.8

[a]T_{peak} was not identified.

observed only slight differences in the DTG curves.[70] Furthermore, the mechanism of lignin pyrolysis is more complex than those of cellulose and hemicellulose, which involve the depolymerization into oligomers. Besides the depolymerization process, it also includes free radical and chain propagation reactions that continue until the stable compounds are formed.[69] The TG profile along with the FTIR characterization suggest that the mass losses observed during the TG curve in LRM can be ascribed almost exclusively to lignin, lignin oligomers, or a mixture thereof. The corresponding mass loss due to the moisture content for LRM was 7.8%. This was followed by two overlapped peaks observed in step II (T_{peak1} = 198 °C with mass loss = 12.6% and T_{peak2} = 258 °C with mass loss = 20.3%, Table 3 and Figure 7b) accounting for lignin depolymerization into oligomers that decompose at a lower temperature.[69] LRM also displayed an overlapping peak, accounting for a mass loss of 14.2% (T_{peak} = 315 °C), which corresponds to step III and is in agreement with a low cellulose content.

To get a closer insight into the actual composition of the different solid fractions obtained from the CSW, a prediction model was followed. Recently, the three parallel reaction model combined with the distributed activation energy model (DAEM) has been used to predict the biomass composition because it is considered a reliable model to describe the pyrolysis of biomass.[43,45] The three parallel-DAEM model assumes three independent first-order reactions of the three pseudocomponents of biomass, usually hemicellulose, cellulose, and lignin. Each pseudocomponent has an activation energy with a Gaussian distribution and a specific frequency factor. The initial composition of biomass is then estimated based on the assumption that each pseudocomponent can be decomposed completely at the final temperature of the pyrolysis. Herein, we present the application of the first-order three parallel-DAEM model based on the mass loss TG data (eq 1 in Materials and Methods) of CSW-derived biomasses obtained via treatment with DESs and ILs. Further description of the model is reported elsewhere[44,73] while our simulation details are given in the Materials and Methods section. Our aim was to assess the initial composition of the different samples to further support our findings on the use of ChCl:Oax2H$_2$O for polyphenols and lignin extraction and ChGly for lignin and cellulose separation.

Figures S22 and S23 (see Supporting Information) show the TG and DTG curves obtained by the mass loss fitting using the first-order three-parallel-DAEM reaction model for CSW and CSWR, and for CRM and LRM, respectively. The optimal values of the full set of parameters (12 parameters for each biomass) calculated simultaneously through the stochastic optimization strategy are listed in Table S3 (see Supporting Information). The fitting quality ranges from 0.308 to 0.527 (Table S3, see Supporting Information) indicating a good fit

(lower FQ indicates a better fitting quality) to the optimization strategy presented here for all biomasses investigated. The fitting quality was similar to that reported for the application of the three parallel-DAEM model by Chen et al.[44] (FQ = 0.37–0.69) for lignocellulosic feedstocks, by Wang et al.[73] (FQ of about 1.65–2.21) for extractive tobacco stem, and by Cai et al.[43] (FQ ranging from 1.57 to 4.45) for lignocellulosic feedstocks. Figures S22 and S23 also depict an excellent fit for all biomasses with residuals between the observed and calculated mass data in the range of 10^{-5} to 10^{-4} values. The kinetic pyrolysis of biomasses derived from chestnut shells can be, therefore, well described by the three parallel-DAEM reaction model.

Figure 8 shows the estimated composition of hemicellulose/cellulose and lignin (the full set of composition values is listed
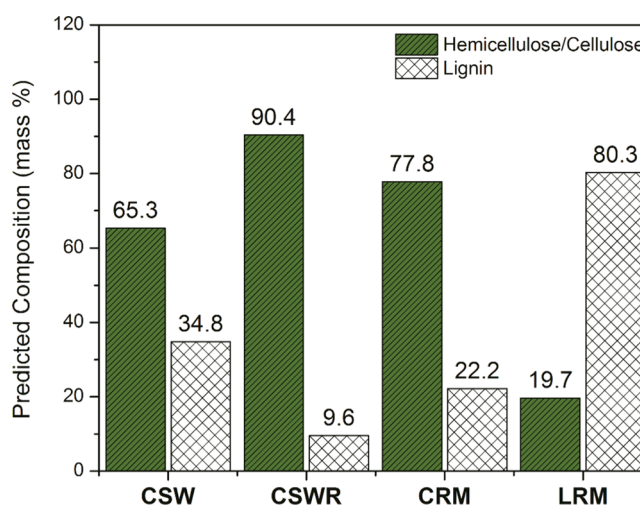

Figure 8. Predicted composition of biomass components in CSW and after the treatment with ChCl-Oax2H$_2$O (CSWR) and ChGly (CRM and LRM) using the three parallel-DAEM model.

in Table S3). The hemicellulose/cellulose content (sum of cellulose and hemicellulose) and the lignin content for CSW, CSWR, and CRM shown in Figure 8 were calculated once the decomposition zone was identified through the analysis of the TG/DTG calculated curves (Figure S22 and S23, see Supporting Information) and through the activation energies (usually following the trend E_0 lignin > E_0 cellulose > E_0 hemicellulose) for each pseudocomponent (1 = hemicellulose, 2 = cellulose, and 3 = lignin). In the case of LRM, we presented the lignin content as the sum of lignin and lignin oligomer (identified as pseudo components: 1 = lignin oligomers, 2 = cellulose, and 3 = lignin) composition in Table S3 (see Supporting Information). These considerations were taken into account because the treatment with

ChCl:Oax2H$_2$O or ChGly could modify the typical decomposition steps (temperature ranges) of the biomass components.

The starting CSW showed a high content of lignin (38.7%) and cellulose (52.5%) and a low hemicellulose (8.8%) content (Table S3, see Supporting Information). The composition values predicted using the three parallel-DAEM model for CSW are then similar to those reported [raw chestnut shells waste: hemicellulose (7.9%), cellulose (28.4%), and lignin (41.6%)] by Morana et al.,[74] highlighting the good predictive power of the model. On the other hand, the lignin composition in CSWR was remarkably lower (6.7%) than that in pristine CSW. These results support the idea that not only high amounts of phenolic compounds (polyphenols and tannins) are extracted during the ChCl:Oax2H$_2$O treatment but lignin is also removed from the lignocellulosic substrate. This is also in good agreement with the extraction mechanism process of lignin from lignocellulosic biomass using ChCl:Oax2H$_2$O reported by different research groups.[52−59] In terms of the amount of cellulose (41.2%) and hemicellulose (52.1%) in CSWR, the model predicted high composition of hemicellulose (pseudocomponent 1). It is most likely, however, that both compositions correspond to cellulose or cellulose/hemicellulose mixtures with different properties (i.e., molecular weight, etc.) because of the fact that CSW has less than 10% of hemicellulose. Also, the activation energies for both components are very close (Table S3, see Supporting Information) and the treatment with ChCl:Oax2H$_2$O could partially hydrolyze the initial hemicellulose present. In fact, the calculated mass loss (TG curves) for these two components showed a similar behavior in the temperature range associated with cellulose decomposition (Figure S19, see Supporting Information). On the other hand, as expected, the biomass obtained after the treatment with ChGly showed high amounts of cellulose/hemicellulose (77.8%) for CRM and lignin (80.3%) for LRM (Figure 8). These results, in agreement with the FTIR data and TG analysis, confirmed that the selected bio- IL ChGly is able to extract lignin from CSWR and hence it allows for the obtainment of cellulose-enriched and lignin-enriched materials.

CONCLUSIONS

In this study, we combined the use of two classes of green solvents, namely DESs and ILs, for the valorization of an agricultural waste with a low economic value (CSW) obtained from a company processing chestnuts. Indeed, such a waste can be reused for producing energy supply, but the elevated humidity of the waste reduces the efficiency of the entire process. First, the ability of a series of DESs to extract from CSW high value-added compounds like polyphenols was screened. Most of these DESs can be classified as NADES with full rights. The results were compared with those obtained with a classical extraction protocol based on the use of MeOH/H$_2$O. The polyphenol extraction efficiency decreased in the following order: acid-based DESs > sugar-based DESs > polyol-based DESs, which correlates well with the α Kamlet−Taft parameter trend. Within the best performing acid-based DESs, ChCl:Oax2H$_2$O displayed the highest capacity of polyphenol extraction, which compared favorably with classical methods. The obtained extracts were analyzed by HPLC and several components were identified and quantified in all the extracts. To the best of our knowledge, this is the first report that uses DESs as solvents for polyphenol extraction from CSW.

Besides demonstrating the utility of DESs in the extraction of polyphenols, a successful attempt to fractioning further the DES-treated CSW was carried out by using a bio-IL, cholinium glycinate. Cellulose-rich and lignin-rich fractions were obtained and analyzed by TGA and FTIR. Furthermore, the three parallel-DAEM reaction model was fitted to the TG pyrolysis profiles of pristine CSW, ChCl:Oax2H$_2$O-treated CSW, cellulose-rich, and lignin-rich materials through a stochastic optimization strategy. Using this method, the composition of cellulose/hemicellulose and lignin was also estimated for each material. The results are in agreement with the literature reports for what concerns the composition of raw CSW in reasonable composition ranges. Considering the positive results of the recycling tests for ChCl:Oax2H$_2$O and of the recovery of ChGy, the proposed approach paves the way for a full exploitation of chestnut shells by using harmless and environmentally friendly solvents and, more in general, for the combined use of DESs and ILs in biomass waste processing.

ASSOCIATED CONTENT

Supporting Information

The Supporting Information is available free of charge at https://pubs.acs.org/doi/10.1021/acssuschemeng.0c04945.

> Experimental details, ^{1}H NMR spectra, HPLC chromatogram of polyphenol standards and extracts, TG and DTG curves, and optimized kinetics parameters (PDF).

AUTHOR INFORMATION

Corresponding Author

Lorenzo Guazzelli — *Department of Pharmacy, University of Pisa, 56126 Pisa, Italy;* orcid.org/0000-0003-4655-2946; Email: lorenzo.guazzelli@unipi.it

Authors

Elena Husanu — *Department of Pharmacy, University of Pisa, 56126 Pisa, Italy*

Angelica Mero — *Department of Pharmacy, University of Pisa, 56126 Pisa, Italy*

Jose Gonzalez Rivera — *Department of Pharmacy, University of Pisa, 56126 Pisa, Italy; National Institute of Optics, (INO-CNR)–UOS Pisa, 56124 Pisa, Italy*

Andrea Mezzetta — *Department of Pharmacy, University of Pisa, 56126 Pisa, Italy*

Julian Cabrera Ruiz — *Department of Chemical Engineering, University of Guanajuato, 36050 Guanajuato, Mexico*

Felicia D'Andrea — *Department of Pharmacy, University of Pisa, 56126 Pisa, Italy*

Christian Silvio Pomelli — *Department of Pharmacy, University of Pisa, 56126 Pisa, Italy;* orcid.org/0000-0002-9630-1179

Complete contact information is available at:
https://pubs.acs.org/10.1021/acssuschemeng.0c04945

Author Contributions

∥E.H. and A.M. equally contributed to this work.

Notes

The authors declare no competing financial interest.

■ REFERENCES

(1) Ravindran, R.; Jaiswal, A. K. Exploitation of Food Industry Waste for High-Value Products. *Trends Biotechnol.* **2016**, *34*, 58−69.

(2) European Commission *Cities for Food Systems Innovation and Green Jobs−FOOD 2030 Workshop Outcomes*, 2017.

(3) Vázquez, G.; Pizzi, A.; Freire, M. S.; Santos, J.; Antorrena, G.; González-Álvarez, J. MALDI-TOF, HPLC-ESI-TOF and 13C-NMR Characterization of Chestnut (Castanea Sativa) Shell Tannins for Wood Adhesives. *Wood Sci. Technol.* **2013**, *47*, 523−535.

(4) Campo, M.; Pinelli, P.; Romani, A. Hydrolyzable Tannins from Sweet Chestnut Fractions Obtained by a Sustainable and Eco-Friendly Industrial Process. *Nat. Prod. Commun.* **2016**, *11*, 1934578X1601100.

(5) de Vasconcelos, M. d. C. B. M.; Bennett, R. N.; Quideau, S.; Jacquet, R.; Rosa, E. A. S.; Ferreira-Cardoso, J. V. Evaluating the Potential of Chestnut (Castanea Sativa Mill.) Fruit Pericarp and Integument as a Source of Tocopherols, Pigments and Polyphenols. *Ind. Crops Prod.* **2010**, *31*, 301−311.

(6) Hong, K. H. Effects of a Solvent System on the Functionalities of Wool and Cotton Fabrics Finished in Chestnut (Castanea Crenata) Shell Extract. *Cellulose* **2018**, *25*, 2745−2753.

(7) Rauf, A.; Imran, M.; Abu-Izneid, T.; Iahtisham-Ul-Haq; Patel, S.; Pan, X.; Naz, S.; Sanches Silva, A.; Saeed, F.; Rasul Suleria, H. A. Proanthocyanidins: A Comprehensive Review. *Biomed. Pharmacother.* **2019**, *116*, 108999.

(8) Van Osch, D. J. G. P.; Kollau, L. J. B. M.; Van Den Bruinhorst, A.; Asikainen, S.; Rocha, M. A. A.; Kroon, M. C. Ionic Liquids and Deep Eutectic Solvents for Lignocellulosic Biomass Fractionation. *Phys. Chem. Chem. Phys.* **2017**, *19*, 2636−2665.

(9) Rauber, D.; Dier, T. K. F.; Volmer, D. A.; Hempelmann, R. Electrochemical Lignin Degradation in Ionic Liquids on Ternary Mixed Metal Electrodes. *Z. Phys. Chem.* **2018**, *232*, 189−208.

(10) Konda, N. V. S. N.; Shi, J.; Singh, S.; Blanch, H. W.; Simmons, B. A.; Klein-Marcuschamer, D. Understanding Cost Drivers and Economic Potential of Two Variants of Ionic Liquid Pretreatment for Cellulosic Biofuel Production. *Biotechnol. Biofuels* **2014**, *7*, 86.

(11) Vázquez, G.; Fontenla, E.; Santos, J.; Freire, M. S.; González-Álvarez, J.; Antorrena, G. Antioxidant activity and phenolic content of chestnut (Castanea sativa) shell and eucalyptus (Eucalyptus globulus) bark extracts. *Ind. Crop. Prod.* **2008**, *28*, 279−285.

(12) Choi, Y. H.; van Spronsen, J.; Dai, Y.; Verberne, M.; Hollmann, F.; Arends, I. W. C. E.; Witkamp, G.-J.; Verpoorte, R. Are Natural Deep Eutectic Solvents the Missing Link in Understanding Cellular Metabolism and Physiology? *Plant Physiol.* **2011**, *156*, 1701−1705.

(13) Florindo, C.; Branco, L. C.; Marrucho, I. M. Quest for Green-Solvent Design: From Hydrophilic to Hydrophobic (Deep) Eutectic Solvents. *ChemSusChem* **2019**, *12*, 1549−1559.

(14) Abranches, D. O.; Martins, M. A. R.; Silva, L. P.; Schaeffer, N.; Pinho, S. P.; Coutinho, J. A. P. Phenolic Hydrogen Bond Donors in the Formation of Non-Ionic Deep Eutectic Solvents: The Quest for Type v Des. *Chem. Commun.* **2019**, *55*, 10253−10256.

(15) Vanda, H.; Dai, Y.; Wilson, E. G.; Verpoorte, R.; Choi, Y. H. Green Solvents from Ionic Liquids and Deep Eutectic Solvents to Natural Deep Eutectic Solvents. *C. R. Chim.* **2018**, *21*, 628−638.

(16) Martins, M. A. R.; Pinho, S. P.; Coutinho, J. A. P. Insights into the Nature of Eutectic and Deep Eutectic Mixtures. *J. Solution Chem.* **2019**, *48*, 962−982.

(17) Huang, J.; Guo, X.; Xu, T.; Fan, L.; Zhou, X.; Wu, S. Ionic Deep Eutectic Solvents for the Extraction and Separation of Natural Products. *J. Chromatogr. A* **2019**, *1598*, 1−19.

(18) Wan Mahmood, W. M. A.; Lorwirachsutee, A.; Theodoropoulos, C.; Gonzalez-Miquel, M. Polyol-Based Deep Eutectic Solvents for Extraction of Natural Polyphenolic Antioxidants from Chlorella Vulgaris. *ACS Sustain. Chem. Eng.* **2019**, *7*, 5018.

(19) Mamilla, J. L. K.; Novak, U.; Grilc, M.; Likozar, B. Natural deep eutectic solvents (DES) for fractionation of waste lignocellulosic biomass and its cascade conversion to value-added bio-based chemicals. *Biomass Bioenergy* **2019**, *120*, 417−425.

(20) Grilc, M.; Likozar, B.; Levec, J. Kinetic model of homogeneous lignocellulosic biomass solvolysis inglycerol and imidazolium-based ionic liquids with subsequentheterogeneous hydrodeoxygenation over NiMo/Al$_2$O$_3$ catalyst. *Catal. Today* **2015**, *256*, 302−314.

(21) Bradić, B.; Novak, U.; Likozar, B. Crustacean shell bio-refining to chitin by natural deep eutectic solvents. *Green Process. Synth.* **2019**, *9*, 13−25.

(22) Welton, T. Ionic Liquids: A Brief History. *Biophys. Rev.* **2018**, *10*, 691−706.

(23) Mezzetta, A.; Perillo, V.; Guazzelli, L.; Chiappe, C. Thermal Behavior Analysis as a Valuable Tool for Comparing Ionic Liquids of Different Classes. *J. Therm. Anal. Calorim.* **2019**, *138*, 3335−3345.

(24) Clarke, C. J.; Tu, W.-C.; Levers, O.; Bröhl, A.; Hallett, J. P. Green and Sustainable Solvents in Chemical Processes. *Chem. Rev.* **2018**, *118*, 747−800.

(25) Swatloski, R. P.; Spear, S. K.; Holbrey, J. D.; Rogers, R. D. Dissolution of Cellose with Ionic Liquids. *J. Am. Chem. Soc.* **2002**, *124*, 4974−4975.

(26) Carneiro, A. P.; Rodríguez, O.; Macedo, E. A. Dissolution and Fractionation of Nut Shells in Ionic Liquids. *Bioresour. Technol.* **2017**, *227*, 188−196.

(27) Elgharbawy, A. A.; Alam, M. Z.; Moniruzzaman, M.; Goto, M. Ionic Liquid Pretreatment as Emerging Approaches for Enhanced Enzymatic Hydrolysis of Lignocellulosic Biomass. *Biochem. Eng. J.* **2016**, *109*, 252−267.

(28) Costa, S. P. F.; Azevedo, A. M. O.; Pinto, P. C. A. G.; Saraiva, M. L. M. F. S. Environmental Impact of Ionic Liquids: Recent Advances in (Eco)Toxicology and (Bio)Degradability. *ChemSusChem* **2017**, *10*, 2321−2347.

(29) Dutta, T.; Papa, G.; Wang, E.; Sun, J.; Isern, N. G.; Cort, J. R.; Simmons, B. A.; Singh, S. Characterization of Lignin Streams during Bionic Liquid-Based Pretreatment from Grass, Hardwood, and Softwood. *ACS Sustain. Chem. Eng.* **2018**, *6*, 3079−3090.

(30) Mezzetta, A.; Łuczak, J.; Woch, J.; Chiappe, C.; Nowicki, J.; Guazzelli, L. Surface Active Fatty Acid ILs: Influence of the Hydrophobic Tail and/or the Imidazolium Hydroxyl Functionalization on Aggregates Formation. *J. Mol. Liq.* **2019**, *289*, 111155.

(31) Becherini, S.; Mezzetta, A.; Chiappe, C.; Guazzelli, L. Levulinate Amidinium Protic Ionic Liquids (PILs) as Suitable Media for the Dissolution and Levulination of Cellulose. *New J. Chem.* **2019**, *43*, 4554−4561.

(32) Hou, X.-D.; Liu, Q.-P.; Smith, T.-J.; Li, N.; Zong, M.-H. Evaluation of Toxicity and Biodegradability of Cholinium Amino Acids Ionic Liquids. *PloS One* **2013**, *8*, No. e59145.

(33) Ninomiya, K.; Inoue, K.; Aomori, Y.; Ohnishi, A.; Ogino, C.; Shimizu, N.; Takahashi, K. Characterization of Fractionated Biomass Component and Recovered Ionic Liquid during Repeated Process of Cholinium Ionic Liquid-Assisted Pretreatment and Fractionation. *Chem. Eng. J.* **2015**, *259*, 323−329.

(34) An, Y.-X.; Li, N.; Wu, H.; Lou, W.-Y.; Zong, M.-H. Changes in the Structure and the Thermal Properties of Kraft Lignin during Its Dissolution in Cholinium Ionic Liquids. *ACS Sustain. Chem. Eng.* **2015**, *3*, 2951−2958.

(35) Dai, Y.; Witkamp, G.-J.; Verpoorte, R.; Choi, Y. H. Tailoring Properties of Natural Deep Eutectic Solvents with Water to Facilitate Their Applications. *Food Chem.* **2015**, *187*, 14−19.

(36) Bubalo, M. C.; Ćurko, N.; Tomašević, M.; Kovačević Ganić, K.; Radojčić Redovniković, I. Green Extraction of Grape Skin Phenolics by Using Deep Eutectic Solvents. *Food Chem.* **2016**, *200*, 159−166.

(37) Tao, D.-J.; Cheng, Z.; Chen, F.-F.; Li, Z.-M.; Hu, N.; Chen, X.-S. Synthesis and Thermophysical Properties of Biocompatible Cholinium-Based Amino Acid Ionic Liquids. *J. Chem. Eng. Data* **2013**, *58*, 1542−1548.

(38) Jung, B. S.; Lee, N.-K.; Na, D. S.; Yu, H. H.; Paik, H.-D. Comparative Analysis of the Antioxidant and Anticancer Activities of Chestnut Inner Shell Extracts Prepared with Various Solvents. *J. Sci. Food Agric.* **2016**, *96*, 2097−2102.

(39) Da Costa Lopes, A. M.; Brenner, M.; Falé, P.; Roseiro, L. B.; Bogel-Łukasik, R. Extraction and Purification of Phenolic Compounds from Lignocellulosic Biomass Assisted by Ionic Liquid, Polymeric Resins, and Supercritical CO2. *ACS Sustain. Chem. Eng.* **2016**, *4*, 3357−3367.

(40) Rodrigues, F.; Santos, J.; Pimentel, F. B.; Braga, N.; Palmeira-de-Oliveira, A.; Oliveira, M. B. P. P. Promising New Applications of Castanea Sativa Shell: Nutritional Composition, Antioxidant Activity, Amino Acids and Vitamin e Profile. *Food Funct.* **2015**, *6*, 2854−2860.

(41) Nakamura, Y.; Tsuji, S.; Tonogai, Y. Analysis of Proanthocyanidins in Grape Seed Extracts, Health Foods and Grape Seed Oils. *J. Health Sci.* **2003**, *49*, 45−54.

(42) Jessop, P. G.; Jessop, D. A.; Fu, D.; Phan, L. Solvatochromic parameters for solvents of interest in green chemistry. *Green Chem.* **2012**, *14*, 1245−1259.

(43) Cai, J.; Wu, W.; Liu, R.; Huber, G. W. A Distributed Activation Energy Model for the Pyrolysis of Lignocellulosic Biomass. *Green Chem.* **2013**, *15*, 1331−1340.

(44) Chen, Z.; Hu, M.; Zhu, X.; Guo, D.; Liu, S.; Hu, Z.; Xiao, B.; Wang, J.; Laghari, M. Characteristics and Kinetic Study on Pyrolysis of Five Lignocellulosic Biomass via Thermogravimetric Analysis. *Bioresour. Technol.* **2015**, *192*, 441−450.

(45) Cai, J.; Wu, W.; Liu, R. An Overview of Distributed Activation Energy Model and Its Application in the Pyrolysis of Lignocellulosic Biomass. *Renew. Sustain. Energy Rev.* **2014**, *36*, 236−246.

(46) Florindo, C.; Oliveira, M. M.; Branco, L. C.; Marrucho, I. M. Carbohydrates-Based Deep Eutectic Solvents: Thermophysical Properties and Rice Straw Dissolution. *J. Mol. Liq.* **2017**, *247*, 441−447.

(47) Gutiérrez, M. C.; Ferrer, M. L.; Mateo, C. R.; Monte, F. D.. Freeze-Drying of Aqueous Solutions of Deep Eutectic Solvents: A Suitable Approach to Deep Eutectic Suspensions of Self-Assembled Structures. *Langmuir* **2009**, *25*, 5509−5515.

(48) Saha, S. K.; Dey, S.; Chakraborty, R. Effect of Choline Chloride-Oxalic Acid Based Deep Eutectic Solvent on the Ultrasonic Assisted Extraction of Polyphenols from Aegle Marmelos. *J. Mol. Liq.* **2019**, *287*, 110956.

(49) González-Rivera, J.; Husanu, E.; Mero, A.; Ferrari, C.; Duce, C.; Tinè, M. R.; D'Andrea, F.; Pomelli, C. S.; Guazzelli, L. Insights into Microwave Heating Response and Thermal Decomposition Behavior of Deep Eutectic Solvents. *J. Mol. Liq.* **2020**, *300*, 112357.

(50) Dai, Y.; Row, K. H. Application of Natural Deep Eutectic Solvents in the Extraction of Quercetin from Vegetables. *Molecules* **2019**, *24*, 2300.

(51) Vella, F. M.; Laratta, B.; La Cara, F.; Morana, A. Recovery of Bioactive Molecules from Chestnut (Castanea Sativa Mill.) by-Products through Extraction by Different Solvents. *Nat. Prod. Res.* **2018**, *32*, 1022−1032.

(52) Wang, S.; Li, H.; Xiao, L.-P.; Song, G. Unraveling the Structural Transformation of Wood Lignin During Deep Eutectic Solvent Treatment. *Front. Energy Res.* **2020**, *8*, 48.

(53) Hong, S.; Shen, X.-J.; Pang, B.; Xue, Z.; Cao, X.-F.; Wen, J.-L.; Sun, Z.-H.; Lam, S. S.; Yuan, T.-Q.; Sun, R.-C. In-Depth Interpretation of the Structural Changes of Lignin and Formation of Diketones during Acidic Deep Eutectic Solvent Pretreatment. *Green Chem.* **2020**, *22*, 1851−1858.

(54) Liu, Y.; Chen, W.; Xia, Q.; Guo, B.; Wang, Q.; Liu, S.; Liu, Y.; Li, J.; Yu, H. Efficient Cleavage of Lignin−Carbohydrate Complexes and Ultrafast Extraction of Lignin Oligomers from Wood Biomass by Microwave-Assisted Treatment with Deep Eutectic Solvent. *Chem-SusChem* **2017**, *10*, 1692−1700.

(55) Da Costa Lopes, A. M.; Gomes, J. R. B.; Coutinho, J. A. P.; Silvestre, A. J. D. Novel Insights into Biomass Delignification with Acidic Deep Eutectic Solvents: A Mechanistic Study of β-O-4 Ether Bond Cleavage and the Role of the Halide Counterion in the Catalytic Performance. *Green Chem.* **2020**, *22*, 2474−2487.

(56) Kandanelli, R.; Thulluri, C.; Mangala, R.; Rao, P. V. C.; Gandham, S.; Velankar, H. R. A Novel Ternary Combination of Deep Eutectic Solvent-Alcohol (DES-OL) System for Synergistic and Efficient Delignification of Biomass. *Bioresour. Technol.* **2018**, *265*, 573−576.

(57) Jablonský, M.; Škulcová, A.; Malvis, A.; Šima, J. Extraction of Value-Added Components from Food Industry Based and Agro-Forest Biowastes by Deep Eutectic Solvents. *J. Biotechnol.* **2018**, *282*, 46−66.

(58) Lynam, J. G.; Kumar, N.; Wong, M. J. Deep Eutectic Solvents' Ability to Solubilize Lignin, Cellulose, and Hemicellulose; Thermal Stability; and Density. *Bioresour. Technol.* **2017**, *238*, 684−689.

(59) Hou, X.-D.; Lin, K.-P.; Li, A.-L.; Yang, L.-M.; Fu, M.-H. Effect of Constituents Molar Ratios of Deep Eutectic Solvents on Rice Straw Fractionation Efficiency and the Micro-Mechanism Investigation. *Ind. Crops Prod.* **2018**, *120*, 322−329.

(60) Dwamena, A. K.; Raynie, D. E. Solvatochromic Parameters of Deep Eutectic Solvents: Effect of Different Carboxylic Acids as Hydrogen Bond Donor. *J. Chem. Eng. Data* **2020**, *65*, 640−646.

(61) Liu, Y.; Chen, W.; Xia, Q.; Guo, B.; Wang, Q.; Liu, S.; Liu, Y.; Li, J.; Yu, H. Efficient Cleavage of Lignin−Carbohydrate Complexes and Ultrafast Extraction of Lignin Oligomers from Wood Biomass by Microwave-Assisted Treatment with Deep Eutectic Solvent. *Chem-SusChem* **2017**, *10*, 1692−1700.

(62) Xia, Q.; Liu, Y.; Meng, J.; Cheng, W.; Chen, W.; Liu, S.; Liu, Y.; Li, J.; Yu, H. Multiple hydrogen bond coordination in threecon-stituent deep eutectic solvents enhances lignin fractionation from biomass. *Green Chem.* **2018**, *20*, 2711−2721.

(63) Squillaci, G.; Apone, F.; Sena, L. M.; Carola, A.; Tito, A.; Bimonte, M.; Lucia, A. D.; Colucci, G.; Cara, F. L.; Morana, A. Chestnut (Castanea Sativa Mill.) Industrial Wastes as a Valued Bioresource for the Production of Active Ingredients. *Process Biochem.* **2018**, *64*, 228−236.

(64) Dai, Y.; van Spronsen, J.; Witkamp, G.-J.; Verpoorte, R.; Choi, Y. H. Natural Deep Eutectic Solvents as New Potential Media for Green Technology. *Anal. Chim. Acta* **2013**, *766*, 61−68.

(65) Cao, J.; Chen, L.; Li, M.; Cao, F.; Zhao, L.; Su, E. Efficient Extraction of Proanthocyanidin from Ginkgo Biloba Leaves Employing Rationally Designed Deep Eutectic Solvent-Water Mixture and Evaluation of the Antioxidant Activity. *J. Pharm. Biomed. Anal.* **2018**, *158*, 317−326.

(66) Rodriguez, N. R.; van den Bruinhorst, A.; Kollau, L. J. B. M.; Kroon, M. C.; Binnemans, K. Degradation of Deep-Eutectic Solvents Based on Choline Chloride and Carboxylic Acids. *ACS Sustain. Chem. Eng.* **2019**, *7*, 11521−11528.

(67) Liu, Q.-P.; Hou, X.-D.; Li, N.; Zong, M.-H. Ionic Liquids from Renewable Biomaterials: Synthesis, Characterization and Application in the Pretreatment of Biomass. *Green Chem.* **2012**, *14*, 304−307.

(68) Lan, W.; Liu, C.-F.; Sun, R.-C. Fractionation of Bagasse into Cellulose, Hemicelluloses, and Lignin with Ionic Liquid Treatment Followed by Alkaline Extraction. *J. Agric. Food Chem.* **2011**, *59*, 8691−8701.

(69) Senneca, O.; Cerciello, F.; Russo, C.; Wütscher, A.; Muhler, M.; Apicella, B. Thermal Treatment of Lignin, Cellulose and Hemicellulose in Nitrogen and Carbon Dioxide. *Fuel* **2020**, *271*, 117656.

(70) Manara, P.; Zabaniotou, A.; Vanderghem, C.; Richel, A. Lignin Extraction from Mediterranean Agro-Wastes: Impact of Pretreatment Conditions on Lignin Chemical Structure and Thermal Degradation Behavior. *Catal. Today* **2014**, *223*, 25−34.

(71) Singh, S.; Varanasi, P.; Singh, P.; Adams, P. D.; Auer, M.; Simmons, B. A. Understanding the Impact of Ionic Liquid

Pretreatment on Cellulose and Lignin via Thermochemical Analysis. *Biomass Bioenergy* **2013**, *54*, 276−283.

(72) Carrier, M.; Loppinet-Serani, A.; Denux, D.; Lasnier, J.-M.; Ham-Pichavant, F.; Cansell, F.; Aymonier, C. Thermogravimetric Analysis as a New Method to Determine the Lignocellulosic Composition of Biomass. *Biomass Bioenergy* **2011**, *35*, 298−307.

(73) Wang, C.; Li, L.; Zeng, Z.; Xu, X.; Ma, X.; Chen, R.; Su, C. Catalytic Performance of Potassium in Lignocellulosic Biomass Pyrolysis Based on an Optimized Three-Parallel Distributed Activation Energy Model. *Bioresour. Technol.* **2019**, *281*, 412−420.

(74) Morana, A.; Squillaci, G.; Paixão, S. M.; Alves, L.; La Cara, F.; Moura, P. Development of an Energy Biorefinery Model for Chestnut (Castanea Sativa Mill.) Shells. *Energies* **2017**, *10*, 1504.